

INFRARED REFLECTANCE MEASUREMENTS OF
MISSOURI WATERS FOR WATER QUALITY APPLICATIONS

Richard C. Waring and Marvin R. Querry
Principal Investigators

Wayne E. Holland, Research Associate

Mary D. Hermann and Leonard M. Earls, Students

Department of Physics
University of Missouri-Kansas City

MISSOURI WATER RESOURCES RESEARCH CENTER
University of Missouri

PROJECT NUMBER - A-063-MO

Agreement Number 14-31-0001-3825

Dates 1 June 1972 - 30 June 1973

COMPLETION REPORT

15 August 1973

The work upon which this publication is based was supported in part by funds provided by the United States Department of the Interior, Office of Water Resources Research, as authorized under the Water Resources Act of 1964.

TABLE OF CONTENTS

ABSTRACT	ii
LIST OF FIGURES.	iv
Section	
I. INTRODUCTION AND OBJECTIVES.	1
II. STATEMENT OF PROBLEM	4
III. EXPERIMENTAL TECHNIQUES.	5
IV. EXPERIMENTAL RESULTS	13
V. KRAMERS KRONIG RELATION.	21
VI. OPTICAL CONSTANTS AND PHASE DIFFERENCE	25
VII. ABSOLUTE REFLECTANCE	40
VIII. CONCLUSIONS.	46
REFERENCES	47
APPENDIX	49

ABSTRACT

INFRARED REFLECTANCE MEASUREMENTS OF MISSOURI WATERS FOR WATER QUALITY APPLICATIONS

Richard C. Waring and Marvin R. Querry
Department of Physics
University of Missouri-Kansas City

The relative specular reflectance of laboratory solutions of 3.0 M Sulfuric Acid and 0.5 M Sodium Nitrate was measured in the 2.0 - 20- μ m wavelength region of the infrared. The relative specular reflectance of natural samples of (1) acid mine drainage taken from a ditch leading from the Peabody Mark Twain Mine to Hinkson Creek; (2) surface water runoff from an agricultural test plot which had received a 314 lb/acre application of nitrate fertilizer; and (3) an oil sample from the Mexico, Missouri oil release into the Salt River was measured in the same spectral region. The data was collected using a Perkin Elmer E-14 spectrophotometer and a reflectometer consisting of a Cassegrain unit which collimated the radiant flux to about 18 mrad divergence, a sample holder and a Cassegrain condenser for focusing the radiant flux, reflected by the sample, onto the entrance slit of the monochromator. The angle of incidence was 70°.

The index of refraction, extinction coefficient and phase difference spectrum throughout the 2-20- μ m wavelength region was

determined for the mine drainage, fuel oil, sulfuric acid, sodium nitrate and nitrate runoff samples using the relative reflectance measurements, the optical constants of distilled water and an algorithm for Kramers-Kronig analysis.

The absolute reflectance spectrum of the alluvium and loess was determined using the relative reflectance measurements, the optical constants of distilled water and the Cauchy equation for reflectance.

It is very desirable to make water quality measurements remotely. However before such measurements can be taken the characteristic manner in which aqueous solutions reflect electromagnetic radiation (in the optical properties) must be known. Thus the results obtained from this research are a part of a much larger goal to determine water quality remotely.

LIST OF FIGURES

Figure		Page
1.	Oblique Angle of Incidence Reflectometer.	6
2.	Normal Incidence Reflectometer.	10
3a.	Relative Reflectance of 3.0 M Sulfuric Acid	16
3b.	Relative Reflectance of Hinkson Creek	17
4a.	Relative Reflectance of 0.5 M NaNO_3	18
4b.	Relative Reflectance of Nitrate Runoff.	19
5.	Relative Reflectance of Diesel Fuel	20
6a.	Index of Refraction of 3.0 M Sulfuric Acid.	26
6b.	Extinction Coefficient of 3.0 M Sulfuric Acid . . .	27
6c.	Phase Difference of 3.0 M Sulfuric Acid	28
7a.	Index of Refraction of Hinkson Creek.	29
7b.	Extinction Coefficient of Hinkson Creek	30
7c.	Phase Difference of Hinkson Creek	31
8a.	Index of Refraction of 0.5 M NaNO_3	32
8b.	Extinction Coefficient of 0.5 M NaNO_3	32
8c.	Phase Difference of 0.5 M NaNO_3	33
9a.	Index of Refraction of Nitrate Runoff	34
9b.	Extinction Coefficient of Nitrate Runoff.	35
9c.	Phase Difference of Nitrate Runoff.	36
10a.	Index of Refraction of Diesel Fuel.	37

10b.	Extinction Coefficient of Diesel Fuel	38
10c.	Phase Difference of Diesel Fuel	39
11a.	Absolute Reflectance of Alluvium #1	42
11b.	Absolute Reflectance of Alluvium #2	43
12a.	Absolute Reflectance of Loess #1.	44
12b.	Absolute Reflectance of Loess #2.	45

"INFRARED REFLECTANCE MEASUREMENTS OF
MISSOURI WATERS FOR WATER QUALITY APPLICATIONS"

R.C. Waring and M.R. Querry
Department of Physics
University of Missouri-Kansas City

I. INTRODUCTION AND OBJECTIVES

The research program associated with project A-063-MO had five objectives:

- (1) To measure the reflectance of infrared radiant energy by natural Missouri water samples in the wavelength region from 2-20- μ m.
- (2) Compute the index of refraction and extinction coefficient from the reflectance data.
- (3) To compute the phase difference between electromagnetic waves reflected at the surface of the sample and at the surface of distilled water.
- (4) To compute the concentration of the solute in the natural samples from the phase difference spectra when possible.
- (5) To perform a pilot study to determine if soil types and soil content in aqueous solutions can be found from infrared reflectance techniques.

The following natural samples were investigated.

- (1) Acid mine drainage taken from a ditch leading from the

Peabody Mark Twain Mine to Hinkson Creek.

- (2) Surface water runoff from a University of Missouri-Columbia agricultural test plot which had received an application of nitrate fertilizer.
- (3) An oil sample from the Mexico, Missouri oil spill into the Salt River.

The mine drainage and oil samples were supplied by the Missouri Department of Conservation, Fish and Wildlife Research Center and the nitrate runoff sample was supplied by Dr. George E. Smith, Director, Missouri Water Resources Research Center.

Laboratory solutions of 3.0 M sulfuric acid and 0.5 M sodium nitrate were studied for comparison purposes.

In accordance with objective (5) we determined the reflectance of one alluvium and one loess soil sample containing various amounts of water.

The purpose of this report is to present, in some detail, the results derived from this program. Section II presents a brief statement of the problem. In Section III we present the experimental procedure for making relative reflectance measurements. The relative reflectances of the aqueous solutions are presented in graphical form and the effects of the solutes on the relative reflectance spectra are discussed in Section IV. In Section V the Kramers-Kronig analysis for computing the optical constants and phase difference is outlined as it was applied to the reflectance data. The optical constants and phase difference of the aqueous

solutions are presented in Section VI. Methods for computing the absolute reflectance of the soil samples from relative reflectances are outlined in Section VII. The absolute reflectances of the soil samples are presented in graphical form. Conclusions drawn from this research program are presented in Section VIII. The report ends with a list of publications and presentations derived, in part, from this project and a list of references.

II. PROBLEM

The desirability of routinely measuring the quality of natural waters has increased with increasing sources of industrial and domestic pollutants. Clearly it would be advantageous to monitor water quality remotely; thus avoiding the time consuming and limited usefulness of hand sampling. Before water quality measurements can be made from data collected remotely from infrared systems the characteristic manner in which solutes in water reflect electromagnetic radiation must be known. In this research project we have determined the characteristic way in which some solutes and oil reflect infrared radiation. Thus our research is a part of a larger goal to monitor water quality remotely.

III. EXPERIMENTAL TECHNIQUES

The reflectometer for measuring specular reflectance is an improved design of the reflectometer that Querry et al.^{1/} used in 1968 to measure the specular reflectance of distilled water. This system was operated in the 2-20- μ m wavelength region for all samples except the soils. A diagram of the reflectometer spectrophotometer system is shown in Figure 1. When operating the system in the infrared spectral region, a glower G emits radiant flux which is chopped at C and is then collected and collimated by a Cassegrain unit consisting of spherical mirrors M_1 and M_2 . A partially collimated pencil of radiant flux of about 18 mrad divergence passes horizontally to mirror M_3 , and then enters a Cassegrain condenser unit consisting of spherical mirrors M_5 and M_6 . From the condenser unit a convergent cone of radiant flux, with apex angle of about 75 mrad at the entrance slit of the monochromator, passes through a transmission polarizer consisting of 12 silver chloride plates positioned at the Brewster's angle relative to the system's optical axis. The 12 plate polarizer passes less than .1 per cent of the undesired polarization component. A thermopile detector having a CsI window provides a measure of the spectral energy. Interference filters at the monochromator's exit slit prevent overlapping diffraction orders and scattered radiant flux from reaching the detector. The monochromator, chopper, detector assembly, amplifier, recorder, and scan control are a Perkin-Elmer E System.

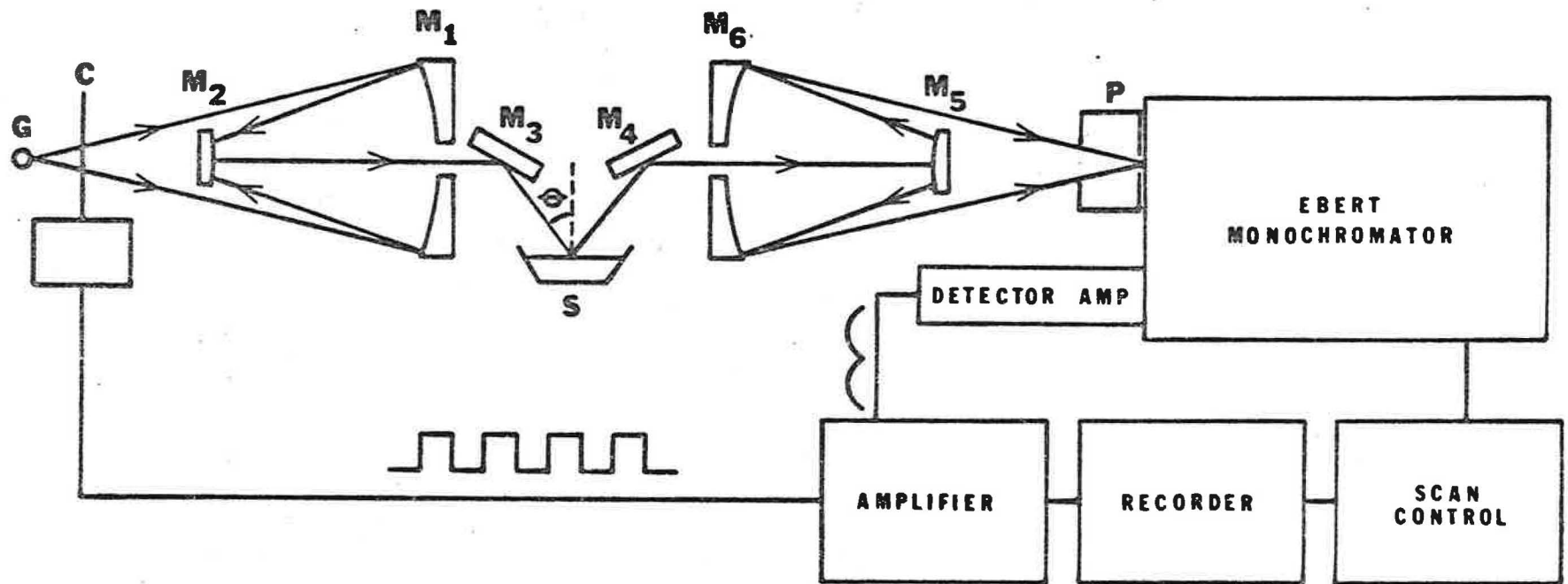


Figure 1.--Oblique Angle of Incidence Reflectometer Spectrophotometer System. The components are a glower G, chopper C, Cassegrain Collimator unit M₁ and M₂, plane mirrors M₃ and M₄, sample S, Cassegrain condenser unit M₅ and M₆, polarizer P, and Perkin Elmer E-system spectrophotometer. The angle of incidence is θ .

The reflectometer was designed and constructed in such a manner that measurements can be made of absolute specular reflectance or of the specular reflectance relative to a calibrated reflectance standard. This technique consistently introduced an additional random error of $\pm 2-3$ per cent in the absolute reflectance measurements. To measure relative specular reflectance, we substitute the reflectance standard for the sample and then carefully move the standard reflector to the sample's original position by adjusting a small laboratory jack while viewing the edge of the reflectance surface through the telescope of a cathetometer. A series of relative reflectance measurements typically have a standard deviation of less than 1.0 per cent. Since the optical constants of distilled water are now known with reasonable certainty^{2-7/} in the 2-20 μm wavelength region of the infrared, we chose distilled water as the reflectance standard and measured the relative reflectance of the aqueous solutions.

The technique for measuring the relative specular reflectance of an aqueous solution for polarized radiant flux was as follows: An aqueous solution was placed at the sample position in the reflectometer. The transmission polarizer was oriented to transmit the H (horizontal polarization) component of radiant intensity I_h and to not transmit the V (vertical polarization) component of radiant intensity I_v . The recorder reading h_s from the spectrophotometer was

$$h_s = m(\tau R_{\perp s} k_h I_h + \ell R_{\parallel s} k_v I_v) , \quad (3-1)$$

where R_{\perp} , R_{\parallel} are respectively the reflectances for radiant flux linearly polarized with the electric field vector perpendicular and parallel to the plane of incidence, τ is the polarizer transmission coefficient, ℓ is the polarizer leakage coefficient, K_h and K_v are characteristic constants of the monochromator and m is a proportionality constant for the detector-amplifier-recorder system. It has been shown^{8/} that (ℓ/τ) is about 0.0006 for two, six plate polarizers in series. For a grating monochromator $1/3 \leq (k_h/k_v) \leq 3$, and for water or weak water solutions $(R_{\perp s}/R_{\parallel s}) \geq 2$ at about 70° angle of incidence which was the angle of incidence for our investigations except for the soil samples. The last term in equation (3-1) was relatively small ($\sim 10^{-3}$); therefore

$$h_s = m a R_{\perp s} k_h I_h. \quad (3-2)$$

Similarly for distilled water placed at the sample position in the reflectometer the recorder reading h_w is given by

$$h_w = m a R_{\perp w} k_h I_h, \quad (3-3)$$

where R_w is the reflectance of the distilled water for horizontally polarized radiant flux. The relative reflectance R_h , the ratio of equation (3-2) to (3-3) is

$$R_h = (h_s/h_w) = (R_{\perp s}/R_{\perp w}). \quad (3-4)$$

We measured h_s and h_w in order to obtain R_h , which is the reflectance of the aqueous solution relative to distilled water for horizon-

tally polarized radiant flux. Measurements of h_s and h_w were alternately repeated until three independent values of R_h were determined in accordance with equation (3-4). The standard deviation of the three values of R_h was then determined by using the theory of errors for a small number of observations. The area of sample covered by radiant flux using the reflectometer at 70° angle of incidence is about 3.5 cm^2 . When collecting data on samples containing 2 grams of soil per liter of water surface ripples, due to stirring, were responsible for non-reproducible data. In an effort to overcome this difficulty and to increase the intensity of the radiant flux at the monochromator we designed and constructed a new, near normal incidence reflectometer. A diagram of this reflectometer spectrophotometer system is shown in Figure 2. A glower G emits infrared radiant flux which is chopped at C, reflected by a plane mirror M_1 to a spherical mirror M_2 which focuses the radiant flux on the sample at an angle of incidence of about 6° . The spherical mirror M_3 collects radiant flux reflected by the sample and focuses it on the entrance slit of the monochromator. The plane mirror M_4 changes the direction of the radiant flux reflected from M_3 . The remainder of the system is the same as in Figure 1 except no polarizer is required.

The difficulties encountered in measuring the relative specular reflectance of soil samples were not completely overcome with the new reflectometer. As a result we measured the relative reflectance of the soils mixed with water in amounts ranging from 26.3 per cent to 35.6 per cent by weight. The technique for measuring the relative

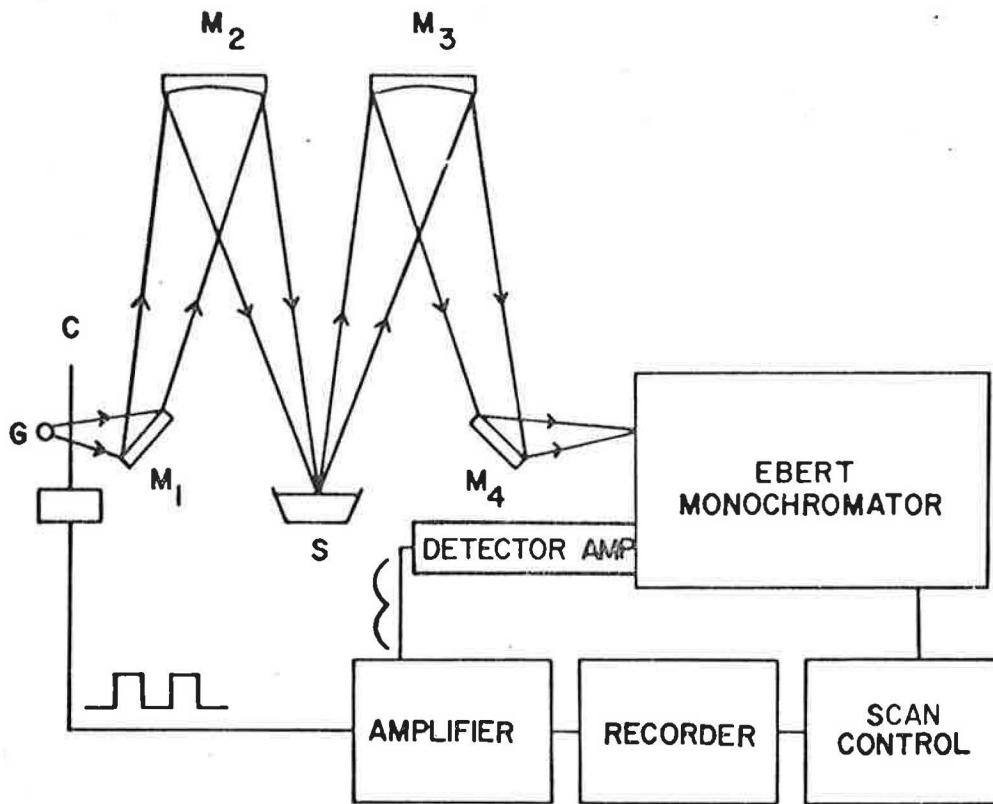


Figure 2.--Near Normal Incidence Reflectometer Spectrophotometer System. The components are a glower G, chopper C, plane mirrors M₁ and M₄, spherical mirrors M₂ and M₃, sample S, and Perkin Elmer E-system spectrophotometer.

reflectance of the soil samples for unpolarized radiant flux is as follows: The sample is placed in the sample position S in Figure 2. The recorder reading h_s is given by

$$h_s = mR_s I \quad (3-5)$$

where m is a proportionality constant for the system, R_s is the reflectance of the sample for unpolarized radiant flux and I is the intensity of the radiation emitted by the source.

For distilled water placed in the sample position the recorder reading h_w is given by

$$h_w = mR_w I \quad (3-6)$$

where R_w is the reflectance of the distilled water for unpolarized radiant flux. The relative reflectance R , the ratio of Eq. (3-5) to (3-6), is

$$R = \frac{h_s}{h_w} = \frac{R_s}{R_w} \quad (3-7)$$

We measured h_s and h_w in order to obtain R , which is the reflectance of the soil sample relative to distilled water. Measurements of h_s and h_w were taken only once since the measurement of h_s was found to depend strongly on the percentage of water in the soil. This percentage decreased with time due to drying of the sample.

The monochromator was operated with spectral slit widths as shown in the table at the end of the report. A cathetometer,

having a protractor ocular as the eye piece for the telescope, was used to measure the angle of incidence θ to about ± 4 mrad for the central ray of the slightly divergent pencil of radiant flux. The angle of incidence for the near normal incidence reflectometer was determined to be $6.0^\circ \pm 0.5^\circ$.

IV. EXPERIMENTAL RESULTS

The experimental techniques outlined in section III were used to measure the relative, infrared reflectance of aqueous solutions of 3.0 M Sulfuric Acid, 0.5 M Sodium Nitrate, and acid mine drainage; (hereafter referred to as Hinkson Creek) and surface water runoff from an agricultural plot which had received a 314 lb/acre nitrate fertilizer application; (hereafter referred to as nitrate runoff.) An oil sample from the Mexico, Missouri oil spill, hereafter referred to as Deisel Fuel was also investigated. Data was collected in the 2-20 μm wavelength region. The data from our relative reflectance measurements are shown graphically in Figures 3a-5. These relative reflectance measurements were made for infrared radiant flux incident at an angle of 70° as measured relative to the vertical and for polarization perpendicular to the plane of incidence.

a) 3.0 M Sulfuric Acid

The relative reflectance spectrum of 3.0 M H_2SO_4 is shown in Figure 3a. The first peak at about 2.8 μm increases to about 1.2 then rapidly decreases to about 0.9. This peak is due to the $\nu_1(\text{A}_1)$ and $\nu_3(\text{E})$ modes of H_3O^+ together with a shifting of the central positions of the $\nu_1(\text{A}_1)$ and $\nu_3(\text{B}_1)$ modes of H_2O . The next peak which increases to about 1.3 near 6.0 μm is due to the $\nu_4(\text{E})$ mode of H_3O^+ . The dominant feature of the relative reflectance spectrum is the large multiple

peak centered at 10 μm ; its origin is the $\nu_3(\text{F}_2)$ mode of SO_4^{-2} and the $\nu_1(\text{A}_1)$, $\nu_3(\text{A}_1)$, $\nu_3(\text{E})$ and $\nu_4(\text{A}_1)$ modes of HSO_4^- . The weaker band at about 17 μm is due to the $\nu_4(\text{E})$ mode of HSO_4^- . A more complete analysis of the 3.0 M H_2SO_4 sample can be found in the appendix.

b) Hinkson Creek

When comparing the Hinkson Creek relative reflectance to H_2SO_4 we note that the scale for the Hinkson Creek is much smaller than H_2SO_4 . The peak at about 2.8 μm is probably due to the $\nu_1(\text{A}_1)$ and $\nu_3(\text{E})$ modes of H_3O^+ and a shift in the central positions of the $\nu_1(\text{A}_1)$ and $\nu_3(\text{B}_1)$ modes of H_2O . The multiple peak at about 10 μm is due to the $\nu_3(\text{F}_2)$ mode of SO_4^{-2} and the $\nu_1(\text{A}_1)$, $\nu_3(\text{A}_1)$, $\nu_3(\text{E})$ and $\nu_4(\text{A}_1)$ mode of HSO_4^- . Other structures are within the limits of experimental error ($\pm .01\text{R}$) and need further investigation.

c) 0.5 M Sodium Nitrate

The relative reflectance spectrum of 0.5 M NaNO_3 , Figure 4a, shows a strong band centered at about 7.2 μm . This band is due to the ν_3 mode of the NO_3^- ion. A weaker band appearing at about 12 μm is probably due to the ν_2 and/or ν_4 mode of NO_3^- .

d) Nitrate Runoff

The relative reflectance spectrum of the nitrate runoff sample is shown in Figure 4b. On comparison of the ordinate

scales of Figures 4a and 4b it is apparent that the concentration of nitrate ions in the nitrate runoff is much less than in the laboratory solution. It appears that the spectral signature centered at about $7.2 \mu\text{m}$ is due to the ν_3 band of NO_3^- . Other signatures appearing in the nitrate runoff spectrum are within the limits of experimental error and may not be due to a solute in the sample. The experimental error is of the order of $\pm .01 R_n$.

e) Diesel Fuel

Figure 5 displays the relative reflectance of the diesel fuel sample. This spectrum resembles that of water except at about $3.2 \mu\text{m}$ and possibly at $6.8 \mu\text{m}$ where there may be infrared active bands due to the oil.

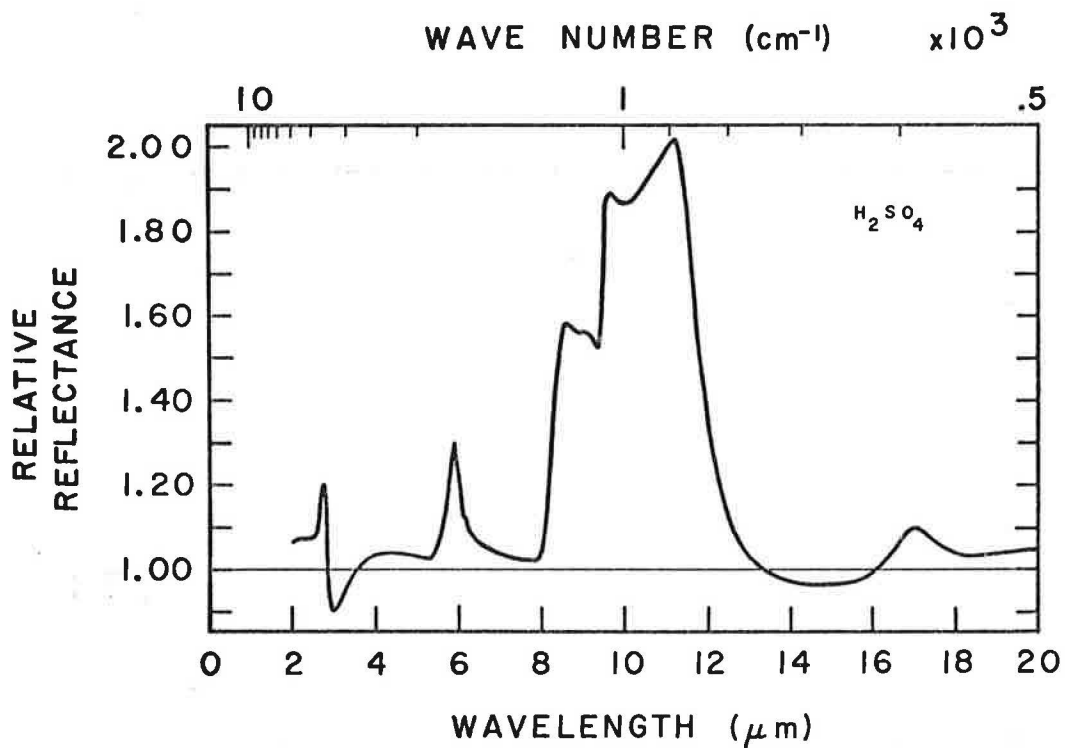


Figure 3a.--The measured and smoothed relative reflectance in the 2-20 μm wavelength region for a 3.0 M aqueous solution of H_2SO_4 . The relative reflectance was measured for horizontally polarized radiant flux incident at $70.03^\circ \pm 0.23^\circ$. Distilled water was the standard mirror. The uncertainty in the measurements was about $.01 R_h$.

HINKSON CREEK

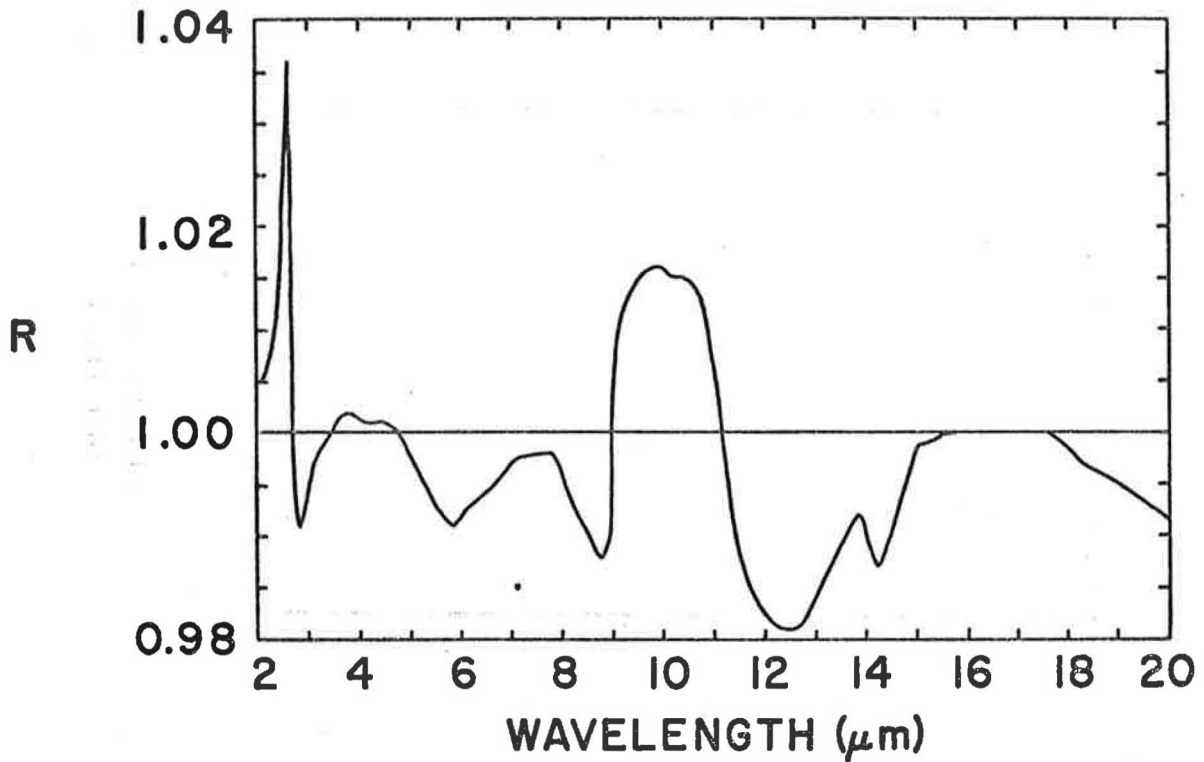


Figure 3b.--The measured and smoothed relative reflectance in the 2-20 μm wavelength region for a natural sample of acid mine drainage taken from a ditch leading from the Peabody Mark Twain Mine to Hinkson Creek. The relative reflectance was measured for horizontally polarized radiant flux incident at $70.03^\circ \pm 0.23^\circ$. Distilled water was the standard mirror. The uncertainty was about $.01 R_h$.

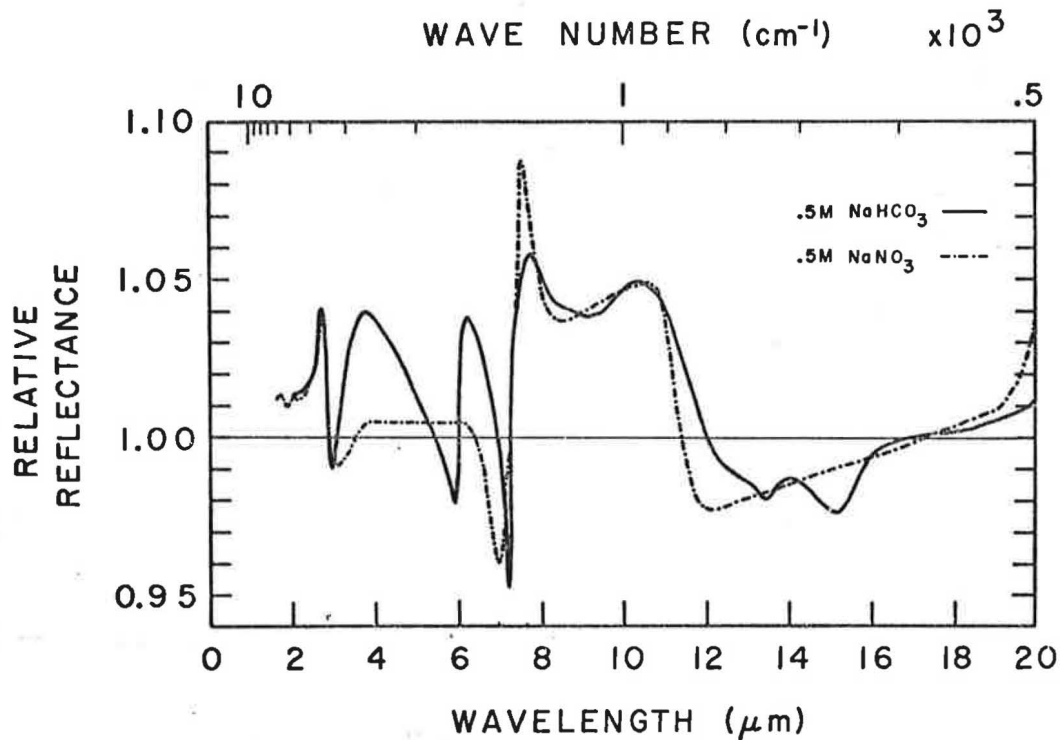


Figure 4a.--The measured and smoothed relative reflectance in the 2-20 μm wavelength region for 0.5 M NaNO_3 $\text{---}\cdot\text{---}\cdot\text{---}\cdot$. The relative reflectance was measured for horizontally polarized radiant flux incident at $70.03^\circ \pm 0.23^\circ$. Distilled water was the reflectance standard. The uncertainty in the measurements was about $.01 R_h$.

NITRATE RUNOFF

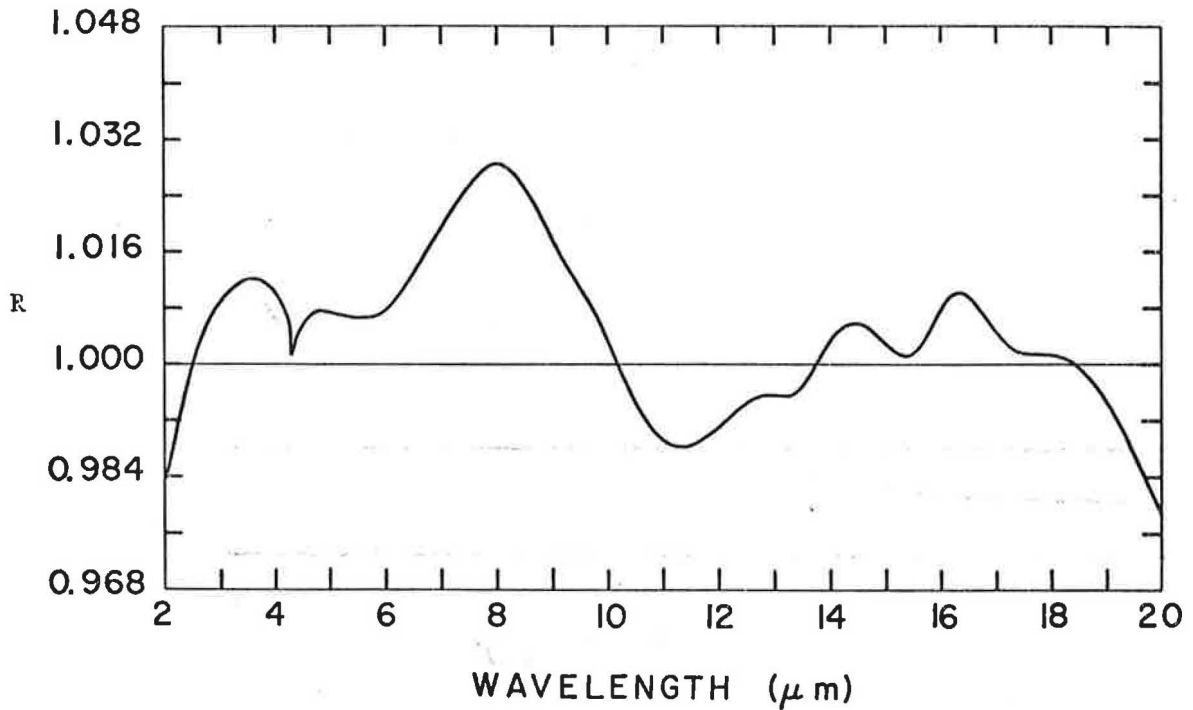


Figure 4b.--The measured and smoothed relative reflectance in the 2-20 μm wavelength region for a natural sample of surface water runoff from an agricultural plot which had received a 314 lb/acre application of nitrate fertilizer. The relative reflectance was measured for horizontally polarized radiant flux incident at $70.03^\circ \pm 0.23^\circ$. Distilled water was the standard mirror. The uncertainty in the measurements was about $.01 R_h$.

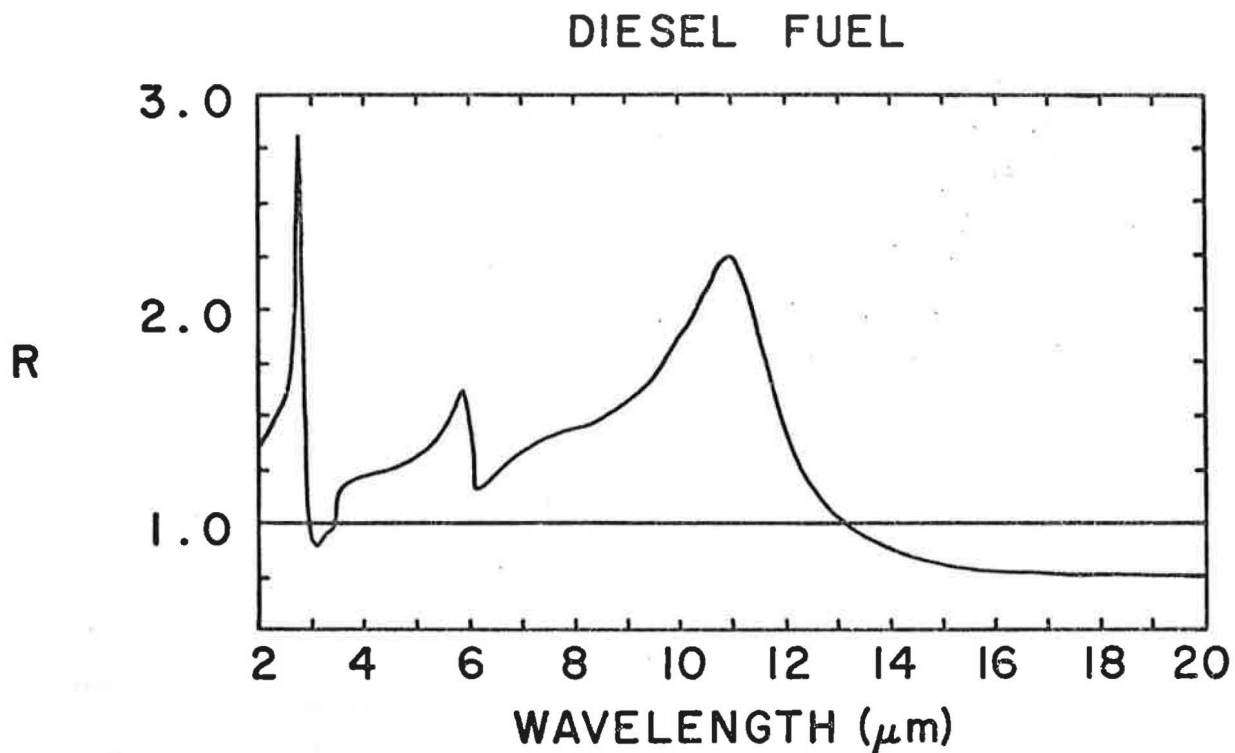


Figure 5.--The measured and smoothed relative reflectance in the 2-20 μm wavelength region for an oil sample from the Mexico, Missouri spill into the Salt River. The relative reflectance was measured for horizontally polarized radiant flux incident at an angle of $70.03^\circ \pm 0.23^\circ$. Distilled water was the standard mirror. The uncertainty in the measurements was about $.01 R_h$.

V. KRAMERS-KRONIG RELATIONS

In this section we present an outline of the Kramers-Kronig analysis which was developed for computing the optical constants of aqueous solutions from their relative reflectance spectrum. Robinson,^{9/} in 1952, was the first to apply what is now known as the Kramers-Kronig (KK) analysis to a reflectance spectrum obtained for infrared radiant flux nearly normally incident on a bulk sample. Subsequent authors^{10-12/} have extended the application of the KK analysis to absolute reflectance spectra obtained for radiant flux that was reflected at an oblique angle and that was linearly polarized either parallel or perpendicular to the plane of incidence. More recently Hale, Holland and Querry^{13/} have developed an algorithm for computing optical constants from a relative reflectance spectrum measured for radiant flux polarized perpendicular to the plane of incidence and reflected at an oblique angle. In this algorithm a KK analysis of the relative reflectance spectra provided the difference $\Delta\phi(\lambda) = \phi(\lambda)_s - \phi(\lambda)_w$ in phase shifts $\phi(\lambda)_s$ and $\phi(\lambda)_w$ for monochromatic waves of wavelength λ reflected at the surface of the aqueous solution s and at the surface of distilled water w , which was used as the reflectance standard. When $\Delta\phi(\lambda)$, the angle of incidence, and the optical constants of the standard reflector were known, the optical constants of the solution could then be determined.

Consider plane electromagnetic waves propagating in vacuum or air to be incident at an angle θ relative to the normal of a plane, infinite, smooth surface of a conducting material medium s that is linear, homogeneous, isotropic, and nonmagnetic. The Fresnel equation for the absolute complex reflectivity $\rho_s e^{-i\phi_s}$ of medium s for waves linearly polarized perpendicular to the plane of incidence is

$$\rho_s e^{-i\phi_s} = (Q_s - iP_s - \cos\theta)/(Q_s - iP_s + \cos\theta), \quad (5-1)$$

where ρ is the modulus of the reflectivity, ϕ_s is the wave's phase shift caused by the reflection, and Q_s and P_s are parameters that are expressed in terms of θ and the material's index of refraction n_s and extinction coefficient k_s as

$$Q_s = \left(\{n_s^2 - k_s^2 - \sin^2\theta + [(n_s^2 - k_s^2 - \sin^2\theta)^2 + 4n_s^2 k_s^2]^{1/2}\} / 2 \right)^{1/2} \quad (5-2)$$

$$P_s = n_s k_s / Q_s. \quad (5-3)$$

The index of refraction is expressed in terms of θ , P_s , and Q_s as

$$n_s = \left(\{Q_s^2 - P_s^2 + \sin^2\theta + [(Q_s^2 - P_s^2 - \sin^2\theta)^2 + 4Q_s^2 P_s^2]^{1/2}\} / 2 \right)^{1/2} \quad (5-4)$$

The extinction coefficient is given by Eq. (5-3). The phase shift $\phi(\lambda)$ may be determined from a KK analysis of an absolute, specular reflectance spectrum for the material;

$$\phi(\lambda) = \text{Prin.} \frac{2\lambda_0}{\pi} \int_0^{\infty} \frac{\ln[\rho_s(\lambda)]}{\lambda^2 - \lambda_0^2} d\lambda, \quad (5-5)$$

where λ is the wavelength, Prin. denotes the Cauchy principal value of the integral, and $\rho_s(\lambda) = R(\lambda)_s^{\frac{1}{2}}$ where $R(\lambda)_s$ is the measured specular reflectance for perpendicularly polarized waves.

The complex relative reflectivity $\rho e^{-i\Delta\phi}$ of the medium s relative to a second medium w for which n_w and k_w are known can be written in two ways for the case of perpendicular polarization

$$\rho e^{-i\Delta\phi} = (\rho_s/\rho_w) \exp[-i(\phi_s - \phi_w)], \quad (5-6)$$

$$\rho e^{-i\Delta\phi} = [(Q_s - iP_s - \cos\theta)(Q_w - iP_w + \cos\theta)] / [(Q_s - iP_s + \cos\theta)(Q_w - iP_w - \cos\theta)]. \quad (5-7)$$

The ratio $\rho_s/\rho_w = R^{\frac{1}{2}}$, where R is the reflectance of medium s measured relative to the reflectance of medium w . The difference in phase shifts $\Delta\phi$ for waves reflected from media s and w is provided by a KK analysis of the relative reflectance spectrum

$$\Delta\phi = \phi_s - \phi_w = \text{Prin.} \frac{\lambda_0}{\pi} \int_0^{\infty} \frac{\ln[R(\lambda)]}{\lambda^2 - \lambda_0^2} d\lambda. \quad (5-8)$$

The quantities Q_w and P_w can be calculated by use of expressions similar to Eqs. (5-2) and (5-3).

Separating Eq. (5-6) into real and imaginary parts and then solving the two resultant equations provides expressions for computing Q_s and P_s

$$Q_s = (A - B) \cos\theta / (A + B - C \cos\Delta\phi - D \sin\Delta\phi), \quad (5-9)$$

$$P_s = (D \cos\Delta\phi - C \sin\Delta\phi) \cos\theta / (A + B - C \cos\Delta\phi - D \sin\Delta\phi) \quad (5-10)$$

where

$$A = (Q_w - \cos\theta)^2 + P_w^2, \quad (5-11)$$

$$B = R[(Q_w - \cos\theta)^2 + P_w^2], \quad (5-12)$$

$$C = 2R^{1/2}(Q_w^2 + P_w^2 - \cos^2\theta), \quad (5-13)$$

$$D = 4R^{1/2}P_w \cos\theta. \quad (5-14)$$

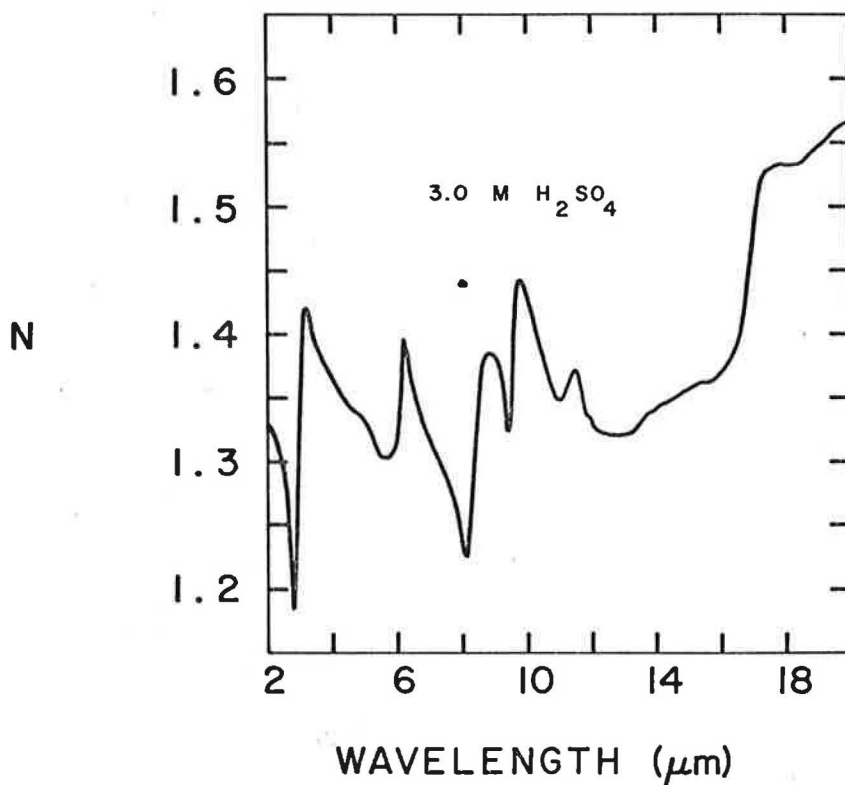
The optical constants n_s and k_s are determined next by use of Eqs. (5-4) and (5-3).

The KK analysis indicated by Eq. (5-8) requires a knowledge of the relative reflectance $R(\lambda)$ for all λ . Because the relative reflectance data were only for the 2-20- μm region, we assumed the relative reflectances were $R(2 \mu\text{m})$ and $R(20 \mu\text{m})$ throughout the $\lambda \leq 2 \mu\text{m}$ and $\lambda \geq 20 \mu\text{m}$ regions, respectively. The integration was made with numerical Simpson's rule techniques in the 2-20- μm region and analytically in the other regions. The parameters Q_w and P_w were determined by use of the optical constants n_w and k_w of distilled water and equations similar to Eqs. (5-2) and (5-3).

VI. OPTICAL CONSTANTS AND PHASE DIFFERENCE

The optical constants of a substance are the index of refraction and the extinction coefficient, i.e. the real and imaginary parts of the complex refractive index. The optical constants and phase difference spectra of the aqueous solution of nitrate and sulfuric acid and of the natural samples and oil were computed according to the Kramers-Kronig analysis outlined in Section V. The results of the computations are shown graphically in Figures 6a-10c.

A knowledge of the optical constants of a substance enables one to compute reflectances and emittances of the substance for any desired geometrical configuration. Therefore, a knowledge of the optical constants is invaluable for a study of the feasibility of detecting remotely the substance from a reflectance or emittance spectrum.



Figures 6a.--The index of refraction (N) in the 2-20 μm wavelength region for a 3.0 M aqueous solution of H_2SO_4 as computed from a Kramers-Kronig analysis of the relative reflectance spectrum for the oblique angle of incidence $70.03^\circ \pm 0.23^\circ$.

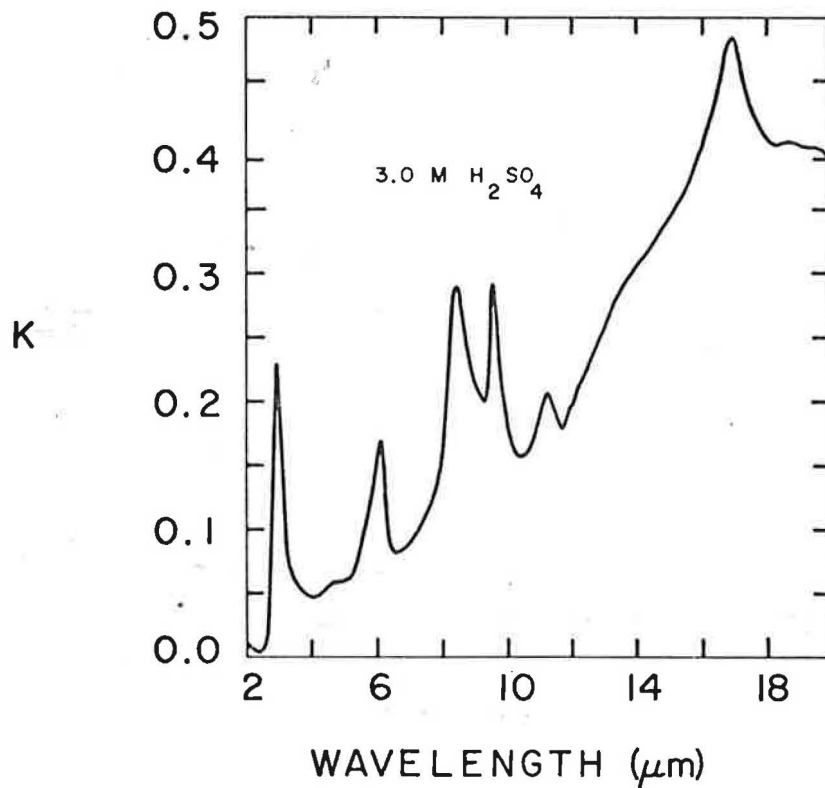


Figure 6b.--The extinction coefficient (K) in the 2-20 μm wavelength region for a 3.0 M aqueous solution of H_2SO_4 as computed from a Kramers-Kronig analysis of the relative reflectance spectrum for the oblique angle of incidence $70.03^\circ \pm 0.23^\circ$.

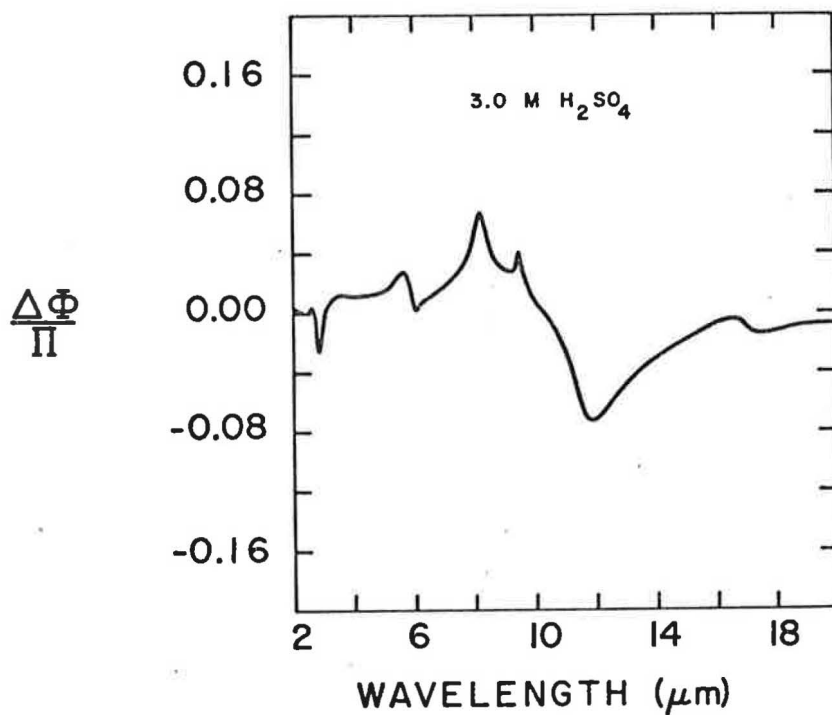


Figure 6c.--The phase difference for electromagnetic waves reflected from an air-H₂SO₄ interface and air-distilled water interface in the wavelength region 2-20 μm. The phase difference was computed from the Kramers-Kronig integral and the relative reflectance spectrum. The angle of incidence was 70.03° ± 0.23°.

HINKSON CREEK

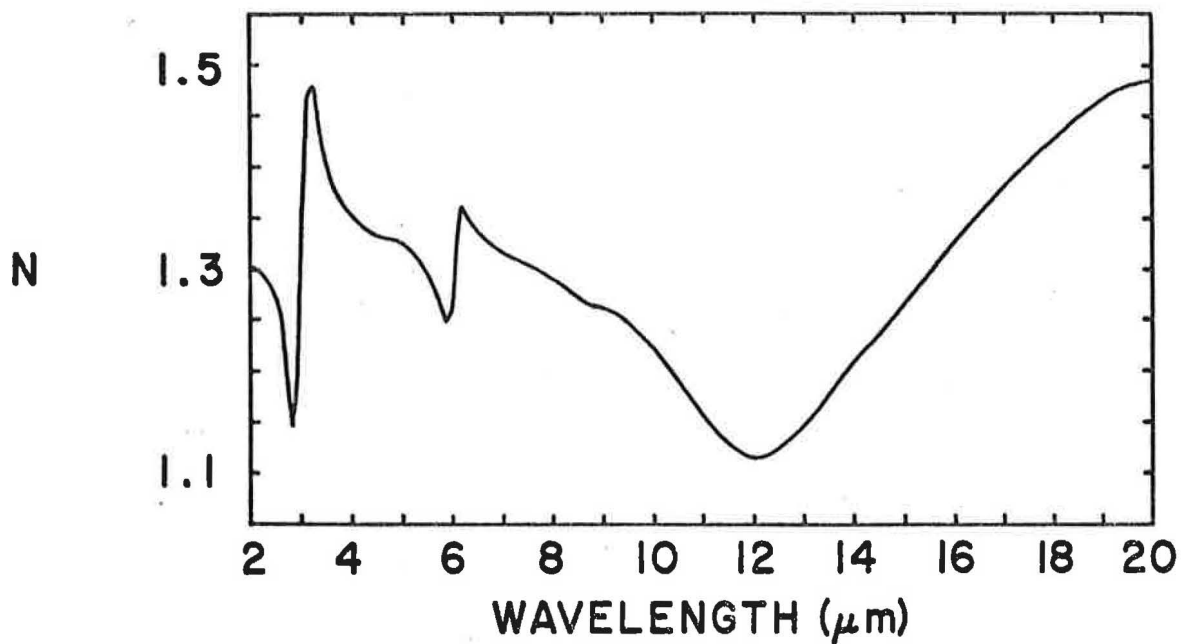


Figure 7a.--The index of refraction (N) in the 2-20 μm wavelength region for the natural sample of acid mine drainage as computed from a Kramers-Kronig analysis of the relative reflectance spectrum for the angle of incidence $70.03^\circ \pm 0.23^\circ$.

HINKSON CREEK

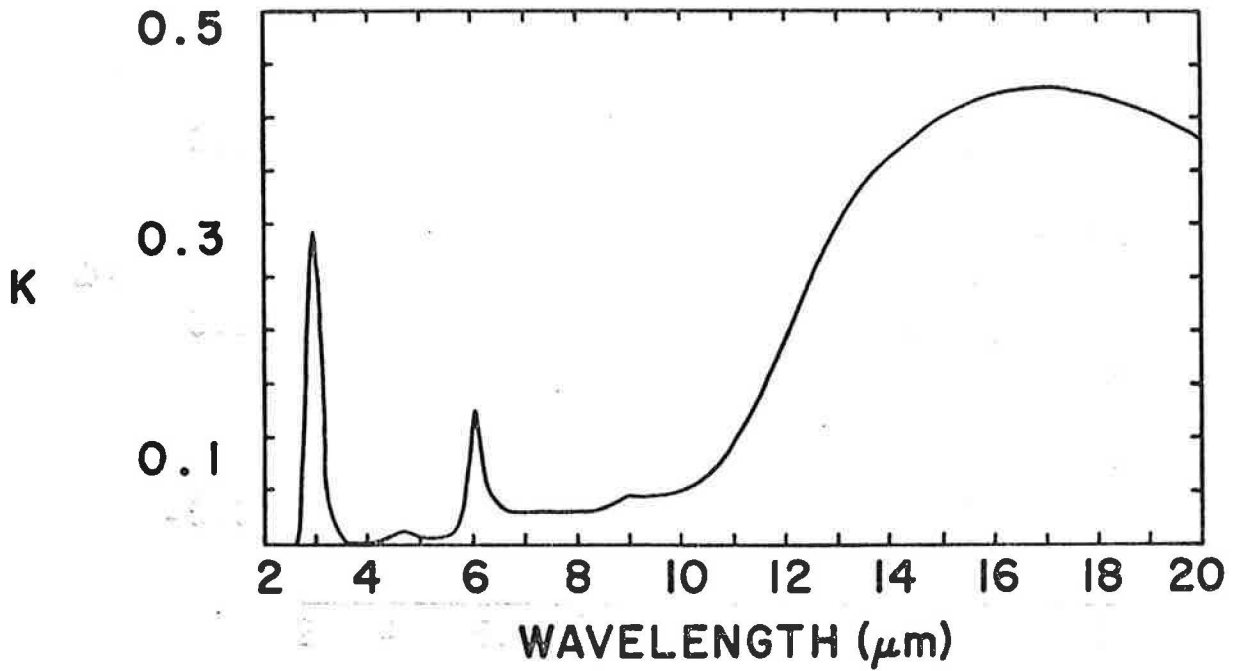


Figure 7b.--The extinction coefficient (K) in the 2-20 μm wavelength region for the natural sample of acid mine drainage as computed from a Kramers-Kronig analysis of the relative reflectance spectrum for the angle of incidence $70.03^\circ \pm 0.23^\circ$.

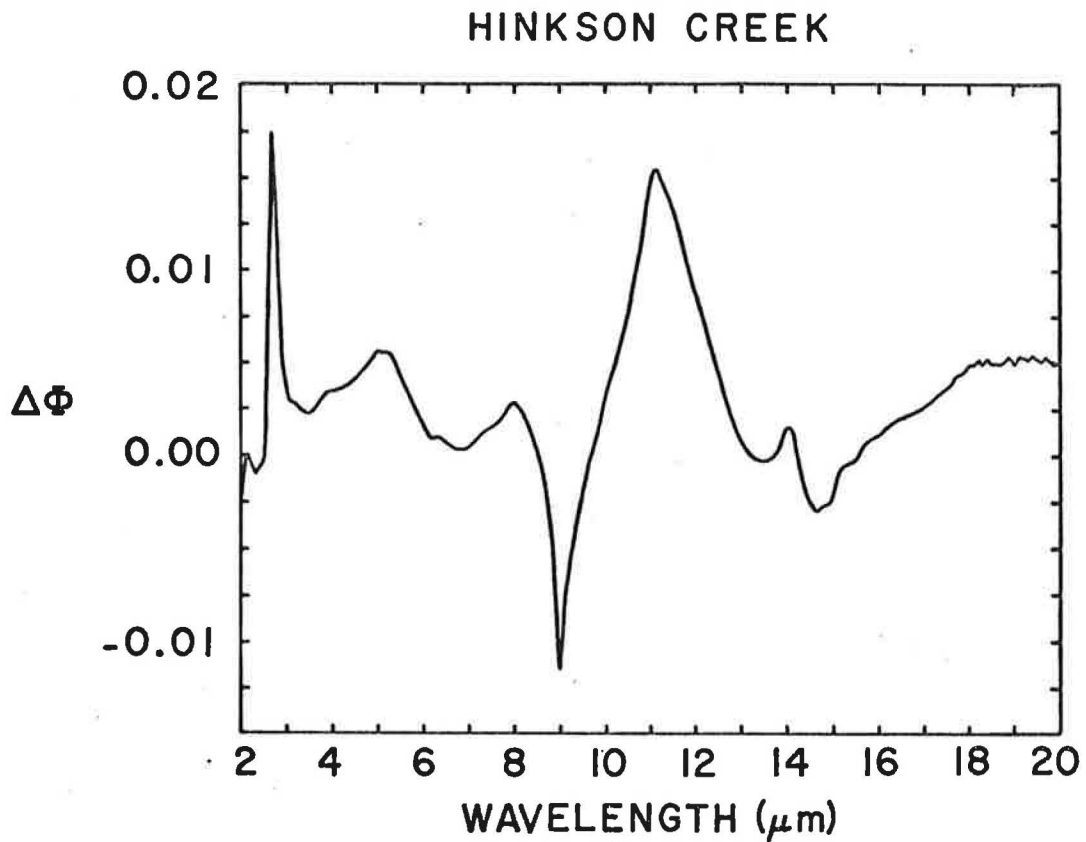


Figure 7c.--The phase difference for electromagnetic waves reflected from an air-acid mine drainage interface and an air-distilled water interface in the 2-20 μm wavelength region. The phase difference was computed from the Kramers-Kronig integral and the relative reflectance spectrum. The angle of incidence was $70.03^\circ \pm 0.23^\circ$.

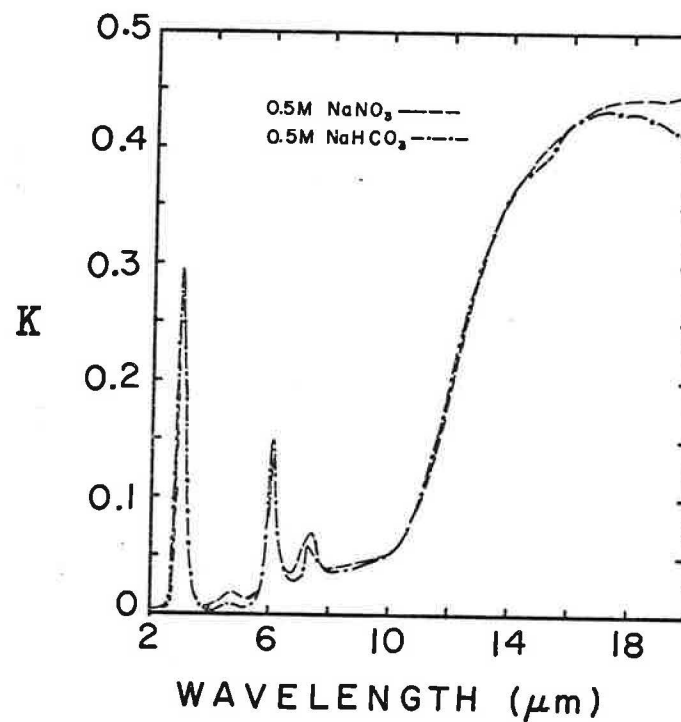
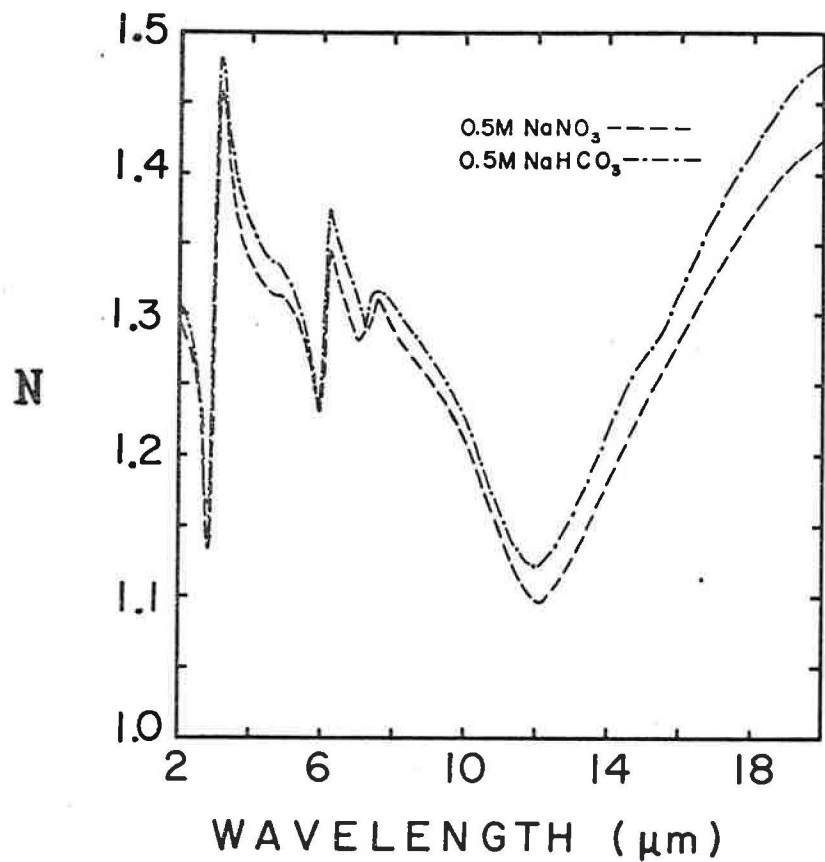


Figure 8a & b.--The index of refraction (N) and extinction coefficient (K) in the 2-20 μm wavelength region for a 0.5 M aqueous solution of NaNO_3 as computed from a Kramers-Kronig analysis of the relative reflectance spectrum for the angle of incidence $70.03^\circ \pm 0.23^\circ$.

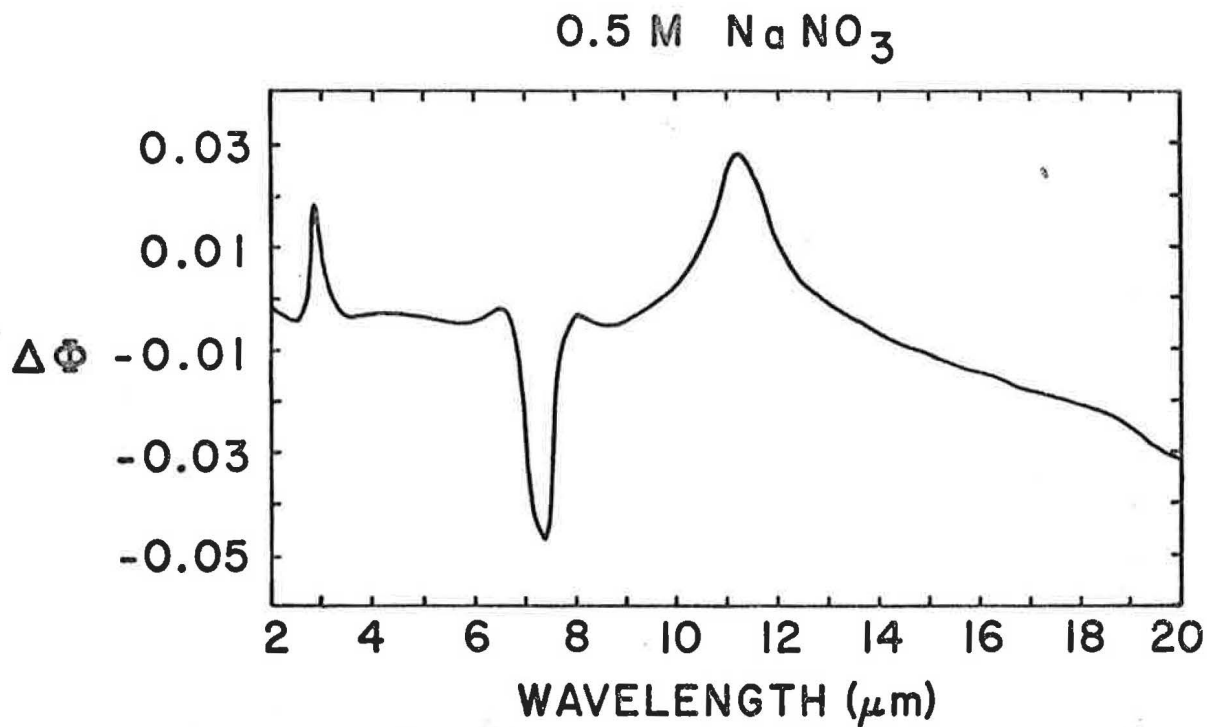


Figure 8c.--The phase difference for electromagnetic waves reflected from an air NaNO_3 interface and an air-distilled water interface in the wavelength region 2-20 μm . The phase difference was computed from the Kramers-Kronig integral and the relative reflectance spectrum. The angle of incidence was $70.03^\circ \pm 0.23^\circ$.

NITRATE RUNOFF

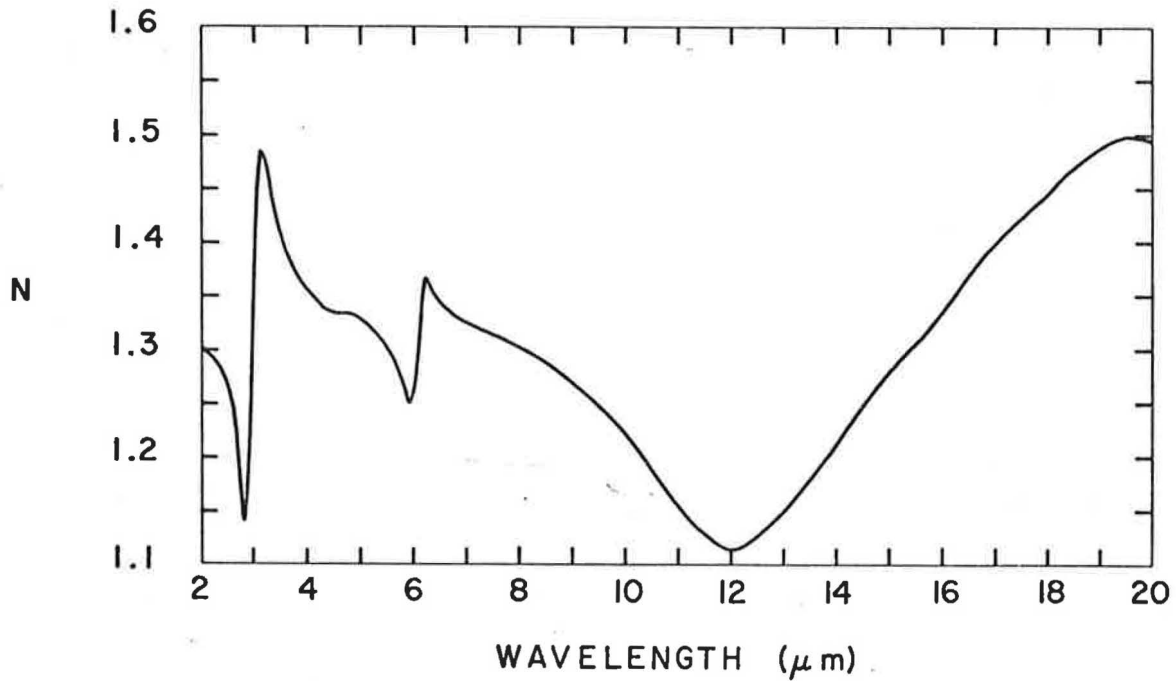


Figure 9a.--The index of refraction (N) in the 2-20 μm wavelength for surface water runoff from an agricultural plot which had received an application of 314 lb/acre of nitrate fertilizer as computed from a Kramers-Kronig analysis of the relative reflectance spectrum for the angle of incidence $70.03^\circ \pm 0.23^\circ$.

NITRATE RUNOFF

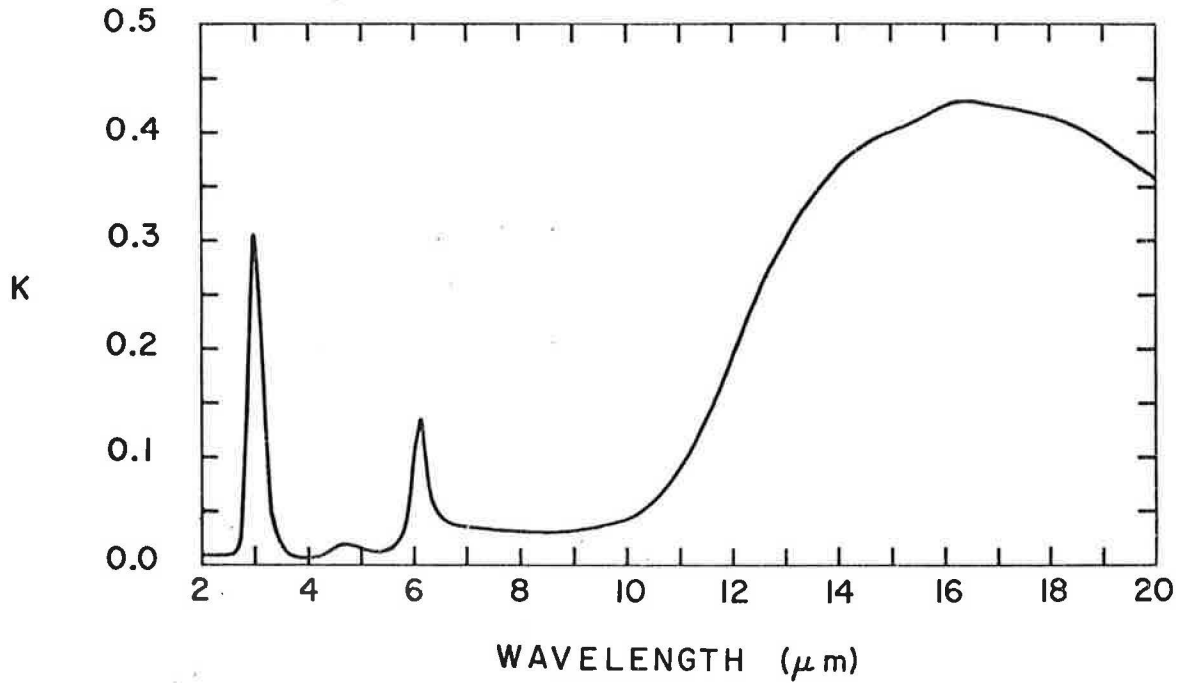


Figure 9b.--The extinction coefficient (K) in the 2-20 μm wavelength for surface water runoff from an agricultural plot which had received an application of 314 lb/acre of nitrate fertilizer as computed from a Kramers-Kronig analysis of the relative reflectance spectrum for the angle of incidence $70.03^\circ \pm 0.23^\circ$.

NITRATE RUNOFF

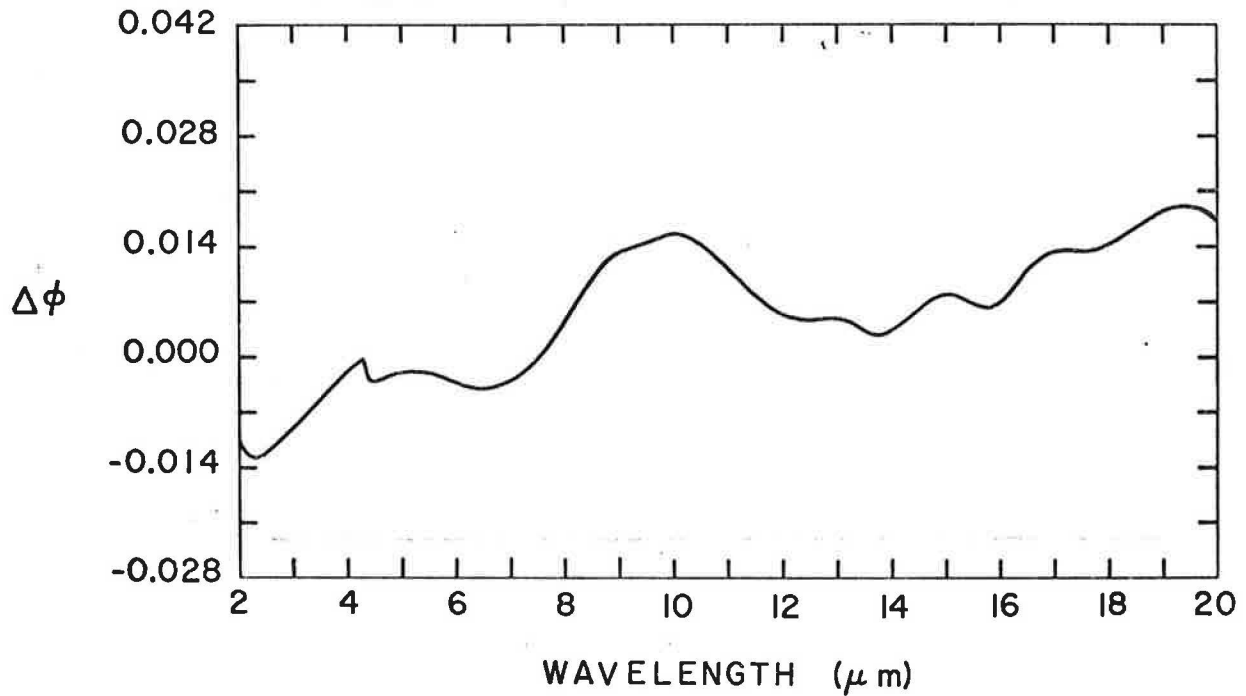


Figure 9c.--The phase difference for electromagnetic waves reflected from an air-agricultural surface water runoff interface and an air-distilled water interface in the wavelength region 2-20 μm . The phase difference was computed from the Kramers-Kronig integral and the relative reflectance spectrum. The angle of incidence was $70.03^\circ \pm 0.23^\circ$.

DIESEL FUEL

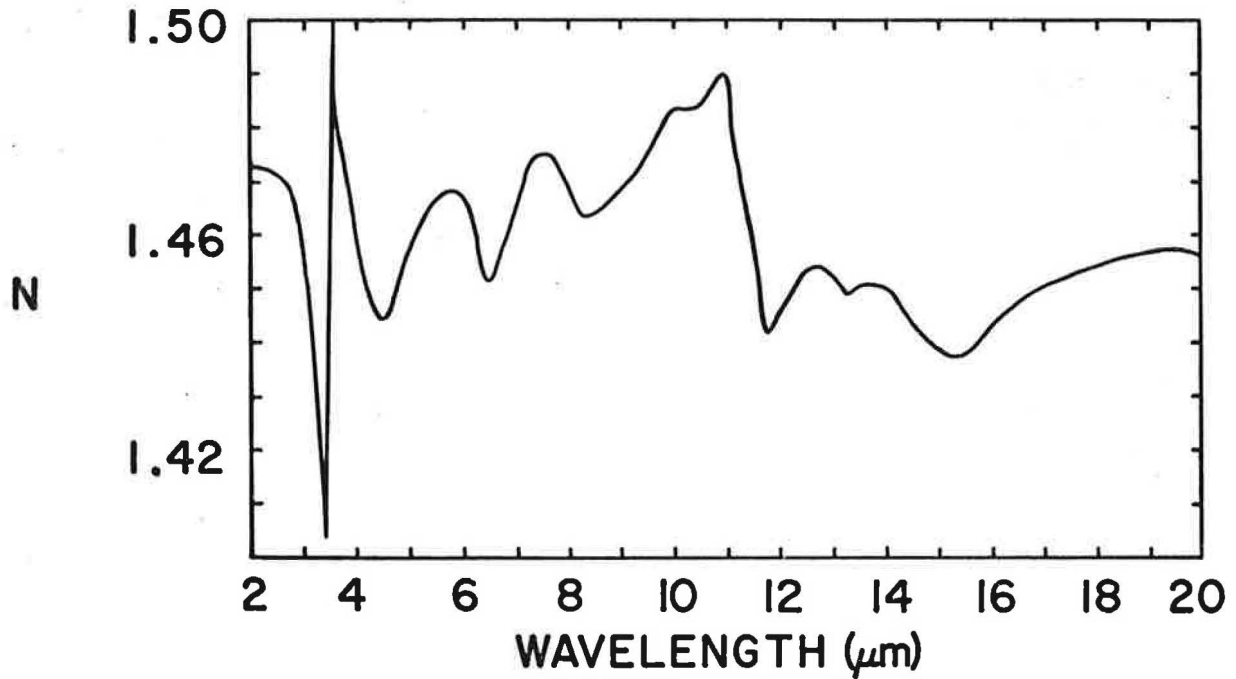


Figure 10a.--The index of refraction (N) in the 2-20 μm wavelength region for an oil sample from the Mexico, Missouri oil spill into the Salt River as computed from a Kramers-Kronig analysis of the relative reflectance spectrum for the angle of incidence $70.03^\circ \pm 0.23^\circ$.

DIESEL FUEL

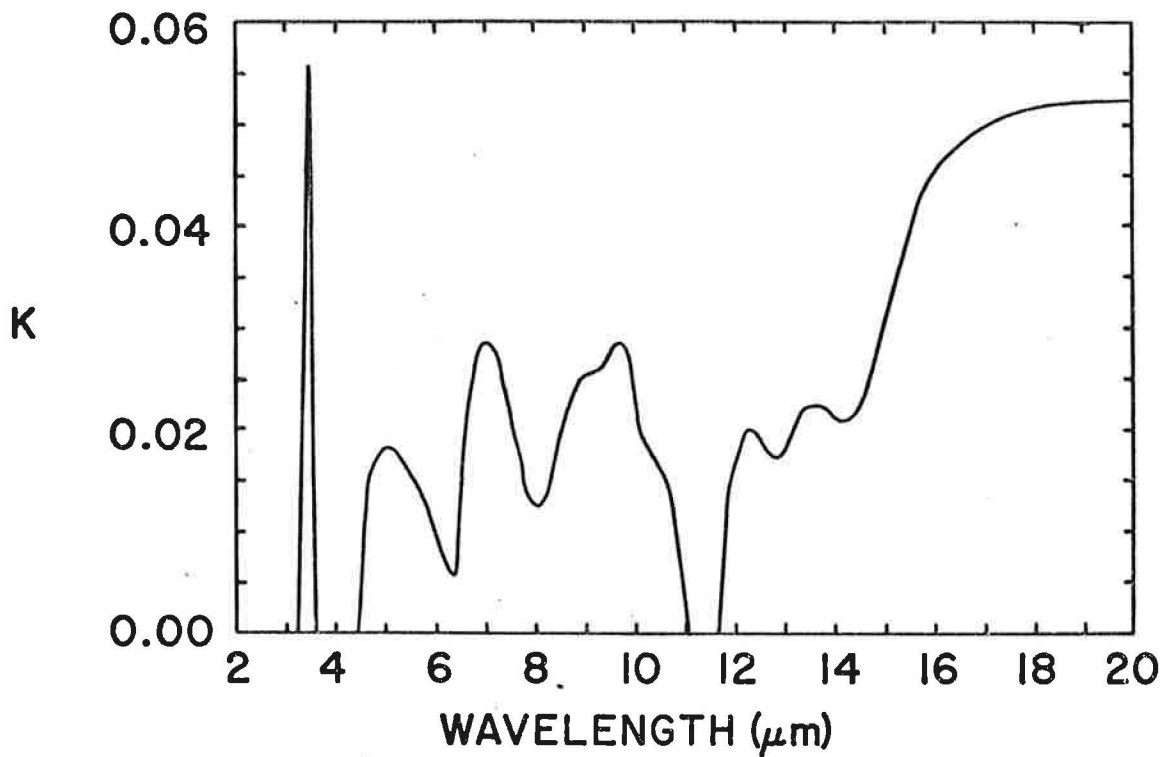


Figure 10b.--The extinction coefficient (K) in the 2-20 μm wavelength region for an oil sample from the Mexico, Missouri oil spill into the Salt River as computed from a Kramers-Kronig analysis of the relative reflectance spectrum for the angle of incidence $70.03^\circ \pm 0.23^\circ$.

DIESEL FUEL

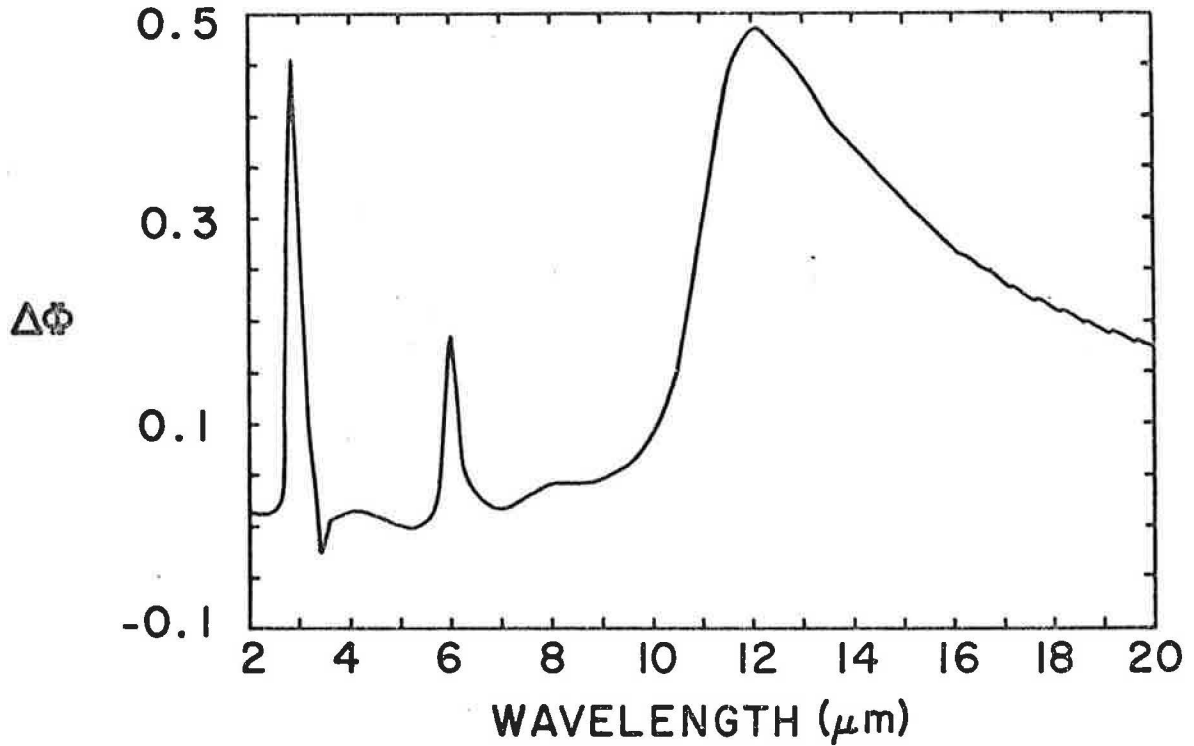


Figure 10c.--The phase difference for electromagnetic waves reflected from an air-Mexico, Missouri oil spill sample interface and an air-distilled water interface in the wavelength region 2-20 μm . The phase difference was computed from the Kramers-Kronig integral and the relative reflectance spectrum. The angle of incidence was $70.03^\circ \pm 0.23^\circ$.

VII. ABSOLUTE REFLECTANCE

This section applies only to the loess and alluvium samples for which we computed the absolute reflectance, Figures 11a-12b, from the measured values of relative reflectance, the Cauchy reflectance equation and the optical constants of distilled water^{7/}. The procedure for computing the absolute reflectance is as follows. We measured R the relative reflectance for aqueous slurry of soils with unpolarized infrared radiant flux at near normal incidence. From equation (3-7) the relative reflectance of the aqueous slurry is

$$R = \frac{R_s}{R_w} \quad (7-1)$$

where R_s and R_w are respectively the absolute reflectance for unpolarized radiant flux at near normal incidence from the surface of the aqueous slurry and from distilled water. The absolute reflectance of the aqueous slurry is therefore

$$R_s = R R_w \quad (7-2)$$

The Cauchy equation describing the absolute reflectance for unpolarized radiant flux at normal incidence as applied to distilled water is

$$R_w = \frac{(n - 1)^2 + k^2}{(n + 1)^2 + k^2} \quad (7-3)$$

where n and k are respectively the index of refraction and extinction coefficients of distilled water. These equations were pro-

grammed on the University's IBM 360/165 computer and the absolute reflectances of the aqueous slurries were computed from equation (7-2) and were then plotted as shown in Figures 11a-12b.

ALLUVIUM # 1

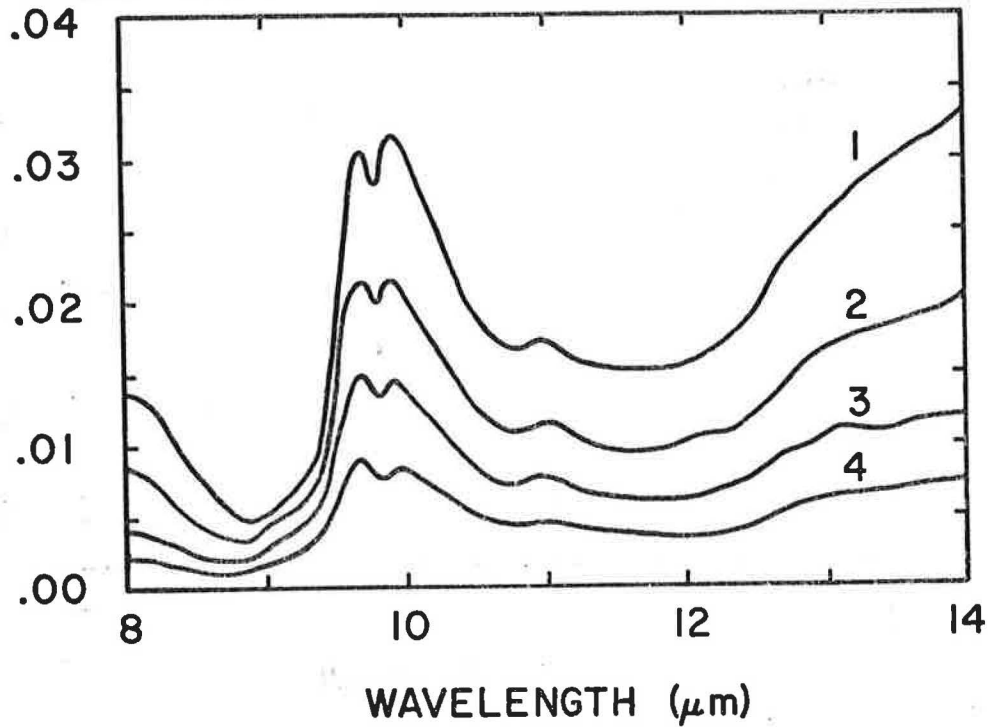


Figure 11a.--The absolute reflectance spectrum of an alluvium aqueous slurry at various moisture contents in the 8-14 μm wavelength region. The absolute reflectance was computed from the relative reflectance spectrum and the optical constants of distilled water. The infrared radiant flux was unpolarized and incident at an angle of $6.0^\circ \pm 0.5^\circ$.

ALLUVIUM # 2

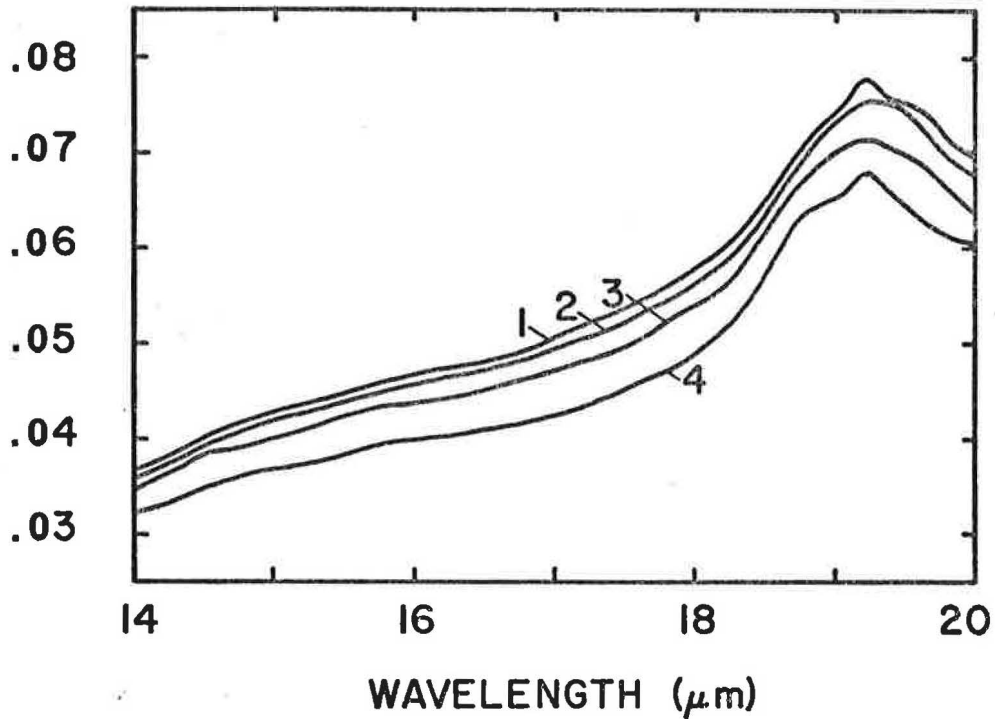


Figure 11b.--The absolute reflectance spectrum of an alluvium aqueous slurry at various moisture contents in the 14-20 μm wavelength region. The absolute reflectance was computed from the relative reflectance spectrum and the optical constants of distilled water. The infrared radiant flux was unpolarized and incident at an angle of $6.0^\circ \pm 0.5^\circ$.

LOESS # 1

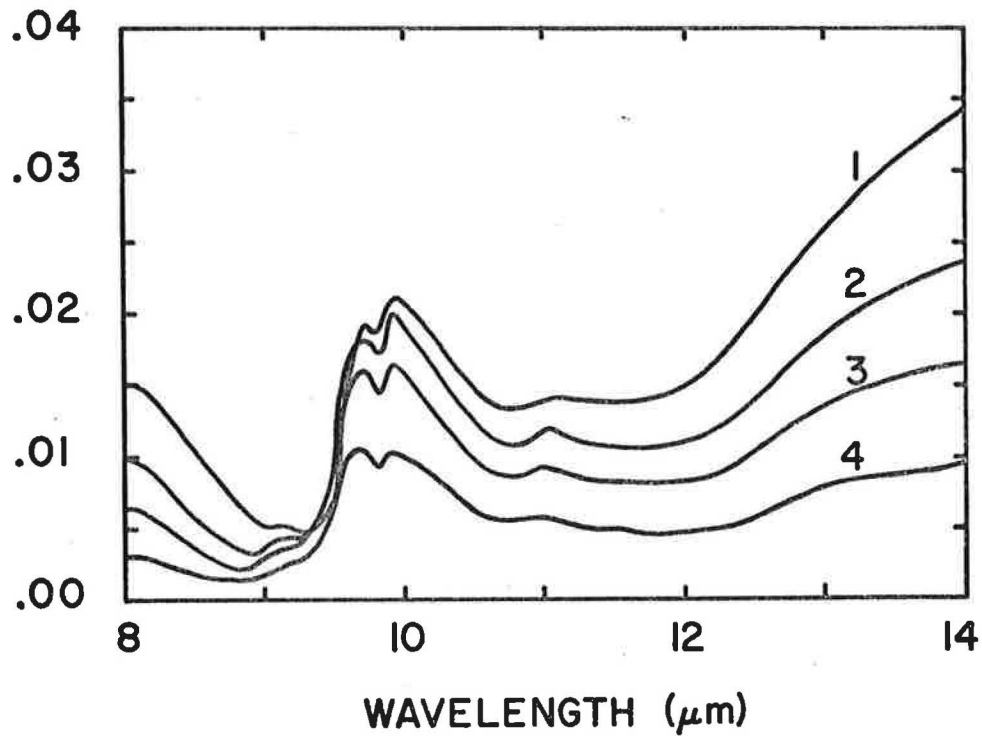


Figure 12a.--The absolute reflectance spectrum of a loess aqueous slurry at various moisture contents in the 8-14 μm wavelength region. The absolute reflectance was computed from the relative reflectance spectrum and the optical constants of distilled water. The infrared radiant flux was unpolarized and incident at an angle of $6.0^\circ \pm 0.5^\circ$.

LOESS # 2

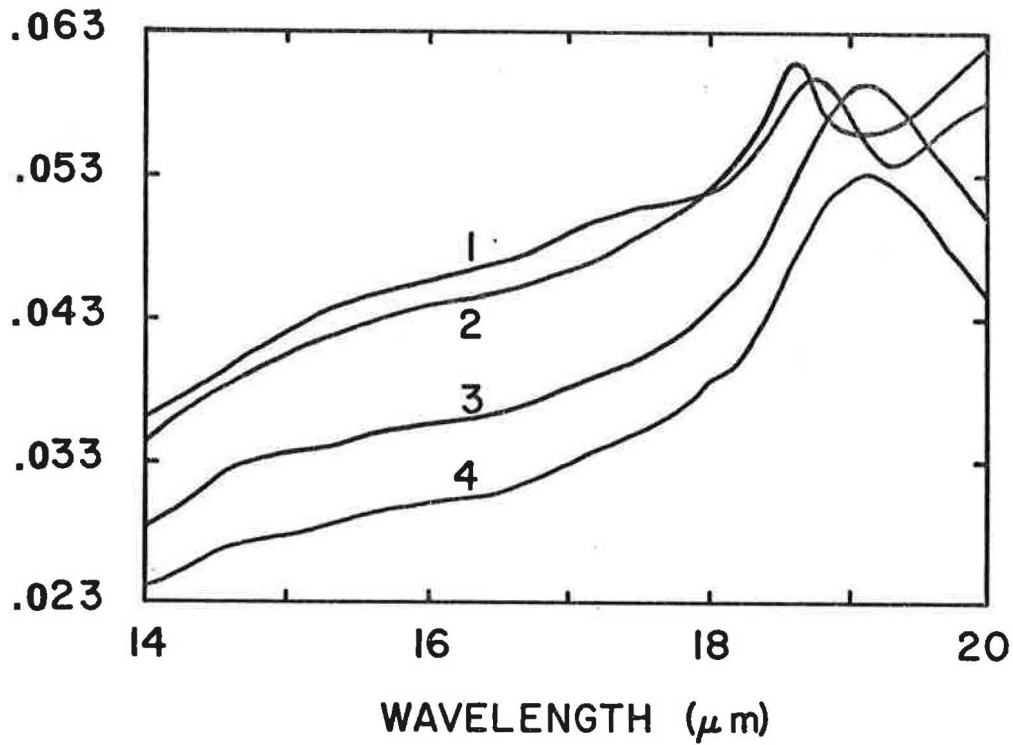


Figure 12b.--The absolute reflectance spectrum of a loess aqueous slurry at various moisture contents in the 14-20 μm wavelength region. The absolute reflectance was computed from the relative reflectance spectrum and the optical constants of distilled water. The infrared radiant flux was unpolarized and incident at an angle of $6.0^\circ \pm 0.5^\circ$.

VIII. CONCLUSIONS

The application of spectral reflectance to qualitatively and quantitatively measure water quality must ultimately use the spectral signatures of the solutes as the basis for the analysis. The relative reflectance spectra of the aqueous solutions studied in this project and others catalogued in our laboratory along with the optical constants and phase differences give us the capability of identifying similar solutes in environmental samples provided the concentration is adequate.

The application of spectral reflectance to the identification of soil types should be pursued further. We studied only two samples and encountered some difficulty in obtaining a specular surface and in maintaining a constant water-soil ratio due to evaporation. Our preliminary results show that moisture content measurements may be feasible by reflectance techniques and should be studied further.

We are grateful for the opportunity to serve the Missouri Water Resources Center. If we can be of further assistance to the Water Resources Center or any other state agency please feel free to contact us. We invite your comments and discussion of the results from this research project.

REFERENCES

1. "Optical Properties of Water in the Infrared," A.N. Rusk, D. Williams, M.R. Querry, Bull. Am. Phys. Soc. 16, 501 (1971).
2. "Infrared Reflectance of Aqueous Solutions of Sulfates and a Phosphate," M.R. Querry, W.E. Holland, R.C. Waring, Bull. Am. Phys. Soc. 16, 502 (1971).
3. "The Reflectance of Aqueous Solutions," M.R. Querry, R.C. Waring, W.E. Holland, and G.R. Mansell, Proceedings 7th International Symposium on Remote Sensing of Environment, University of Michigan (Ann Arbor, May 1971).
4. "Optical Constants of Water in the Infrared," A.N. Rusk, D. Williams, and M.R. Querry, J. Opt. Soc. Am. 61, 895 (1971).
5. "The Infrared Reflectance of Liquid Water," M.R. Querry, Ph.D. Dissertation, Kansas State University (1968).
6. "Refractive Index of Water in the Infrared," M.R. Querry, B. Curnutte, and D. Willaims, J. Opt. Soc. Am. 59, 1299 (1969).
7. "Optical Constants of Water in the Infrared," A. Rusk, D. Williams, and M.R. Querry, J. Opt. Soc. Am. 61, 895 (1971).
8. "The Effect of Herbicides, Pesticides, and Fertilizers on the Optical Properties of Water", M.R. Querry and R.C. Waring, Completion Report OWRR Project No. A-030-MO (1971).
9. T.S. Robinson, Proc. Phys. Soc. (London) A65, 910 (1952).
10. D.M. Roessler, Brit. J. Appl. Phys. 16, 1359 (1965).
11. D.W. Berreman, Appl. Opt. 6, 1519 (1967).
12. M.R. Querry, R.C. Waring, W.E. Holland, G.M. Hale, and W. Nijm, J. Opt. Soc. Am. 62, 849 (1972).
13. G.M. Hale, W.E. Holland, and M.R. Querry, Appl. Opt. 12, 48 (1973).

Spectral Slit Width of Monochromator During Measurements

of Relative Reflectance. λ and ν Respectively

are the Wavelength and Wavenumber.

$\Delta\lambda$ and $\Delta\nu$ respectively are the

Spectral Slit Width in

Units of μm and cm^{-1}

$\lambda(\mu\text{m})$	$\Delta\lambda(\mu\text{m})$	$\nu(\text{cm}^{-1})$	$\Delta\nu(\text{cm}^{-1})$
2.5	10.6	4000	17.0
3.5	23.5	2857	19.2
4.5	54.0	2222	26.7
5.5	52.0	1818	17.2
7.5	46.0	1333	8.2
8.5	42.0	1176	5.8
9.5	38.0	1052	4.2
10.5	135.0	952	12.2
12.5	133.	800	8.5
15.0	126.	667	5.6
17.5	119.	571	3.9
20.0	110.	500	2.8

APPENDIX

The following pages are a preprint of a paper submitted for publication in the Journal of the Optical Society of America and the abstract of a paper presented at the spring meeting of the Optical Society of America.

(1 + r)

ABSTRACT

Reflectance and Optical Constants in the Infrared for NaHCO_3 and NaNO_3 in Water. MARVIN R. QUERRY, W.E. HOLLAND, AND R.C. WARING, Department of Physics, University of Missouri-Kansas City, Kansas City, Mo. 64110.--Relative, specular reflectances of individual 0.5-mole aqueous solutions of NaHCO_3 and NaNO_3 were measured in the $5000\text{-}500\text{-cm}^{-1}$ region of the infrared for the component of radiant flux with the electric-field vector perpendicular to the plane of incidence. Distilled water was the reflectance standard. The angle of incidence was 70° . Kramers-Kronig analyses of the relative reflectance spectra provided phase-difference spectra and values for the optical constants. The strengths of selected infrared bands of HCO_3^- and NO_3^- were determined by numerically integrating values for the molecular extinction coefficients through spectral regions of the bands. The reflectance spectra, optical constants, and molecular extinction coefficients will be presented in graphical form. (13 min.)